Journal of Controlled Release 196 (2014) 9–18

Contents lists available at ScienceDirect

Journal of Controlled Release

journal homepage: www.elsevier.com/locate/jconrel

Targeted cutaneous delivery of ciclosporin A using micellar nanocarriers and the possible role of inter-cluster regions as molecular transport pathways

Maria Lapteva, Verena Santer, Karine Mondon, Ilias Patmanidis, Gianpaolo Chiriano, Leonardo Scapozza, Robert Gurny, Michael Möller, Yogeshvar N. Kalia *

School of Pharmaceutical Sciences, University of Geneva and University of Lausanne, 30 Quai Ernest Ansermet, 1211 Geneva, Switzerland

ARTICLE INFO

Article history:
Received 24 June 2014
Accepted 23 September 2014
Available online 30 September 2014

Keywords:
Psoriasis
Ciclosporin A
Skin topical delivery
Polymeric micelles
Confocal laser scanning microscopy
Transport pathway

ABSTRACT

Oral administration of ciclosporin A (CsA) is indicated in the treatment of severe recalcitrant plaque psoriasis. However, CsA is both nephro- and hepatotoxic and its systemic administration also exposes the patient to other severe side effects. Although topical delivery of CsA, targeted directly to psoriatic skin, would offer significant advantages, there are no topical formulations approved for dermatological use. The aim of this work was to formulate CsA loaded polymeric micelles using the biodegradable and biocompatible MPEG-dihexPLA diblock copolymer and to evaluate their potential for delivering the drug selectively into the skin without concomitant transdermal permeation. Micelle formulations were characterised with respect to drug content, size and morphology. Micelle and drug penetration pathways were subsequently visualised with confocal laser scanning microscopy (CLSM) using fluorescein labelled CsA (Fluo-CsA) and Nile-Red (NR) labelled copolymer. Visualisation studies typically use fluorescent dyes as "model drugs"; however, these may have different physicochemical properties to the drug molecule under investigation. Therefore, in this study it was decided to chemically modify CsA and to use this structurally similar fluorescent analogue to visualise molecular distribution and transport pathways. Molecular modelling techniques and experimental determination of log D served as molecular scale and macroscopic methods to compare the lipophilicity of CsA and Fluo-CsA. The spherical, homogeneous and nanometre-scale micelles (with Z_{av} from 25 to 52 nm) increased the aqueous solubility of CsA by 518-fold. Supra-therapeutic amounts of CsA were delivered to human skin (1.4 ± 0.6 μg/cm^2, cf. a statistically equivalent 1.1 ± 0.5 μg/cm^2 for porcine skin) after application of the formulation with the lowest CsA and copolymer content (1.67 ± 0.03 mg/ml of CsA and 5 mg/ml of copolymer) for only 1 h without concomitant transdermal permeation. Fluo-CsA was successfully synthesised, characterised and incorporated into fluorescent NR-MPEG-dihexPLA micelles; its conformation was not modified by the addition of fluorescein and its log D, measured from pH 4 to 8, was equivalent to that of CsA. Fluo-CsA and NR-MPEG-dihexPLA copolymer were subsequently visualised in skin by CLSM. The images indicated that micelles were preferentially deposited between corneocytes and in the inter-cluster regions (i.e. between the clusters of corneocytes). Fluo-CsA skin penetration was deeper in these structures, suggesting that inter-cluster penetration is probably the preferred transport pathway responsible for the increased cutaneous delivery of CsA.

1. Introduction

Psoriasis is a common skin disease affecting approximately 25 million people in North America and Europe [1]. It is an auto-immune mediated inflammatory disorder in which the mitotic rate of the basal keratinocytes is abnormally high, resulting in erythematous plaques with silvery scales at the skin surface, a thickened epidermis, increased angiogenesis and the presence of inflammatory cells, e.g. dendritic cells, macrophages and T cells in the dermis. Some T cells can also be found in the epidermis [2]. High-potency corticosteroids are the first-line therapeutics used for the topical treatment of psoriasis because of their anti-inflammatory, immunosuppressive and anti-proliferative effects. However, they have many side effects including cutaneous atrophy, formation of telangiectasia, steroid rosacea, perioral dermatitis and increased risk of skin infections to cite but a few [3]. Since the inflammation in psoriasis is strongly related to an excessive immune response, immunosuppressants, such as ciclosporin A (CsA), have shown good efficacy. CsA is a cyclic macrolide undecapeptide that targets T cells present in the dermis and epidermis. It inhibits calcineurin

* Corresponding author at: School of Pharmaceutical Sciences, University of Geneva, 30 Quai Ernest Ansermet, 1211 Geneva 4, Switzerland. Tel.: +41 22 379 3355; fax: +41 22 379 3360.
E-mail address: Yogi.Kalia@unige.ch (Y.N. Kalia).

http://dx.doi.org/10.1016/j.jconrel.2014.09.021
0168-3659/

phosphatase, which is responsible for the translocation of the nuclear factor of activated T cells (NFAT) from the cytoplasm to the nucleus where it promotes the transcription and expression of interleukin-2 and other cytokines.

CsA was the first immunosuppressant to reach the market in 1983 under the trade name of Sandimmune® and later Neoral®. It is currently indicated in the treatment of severe recalcitrant psoriasis when administered orally [4]. Liu et al. [5] demonstrated in rats *in vivo* that CsA applied topically using a bicontinuous microemulsion yielded 30-fold higher drug deposition in skin as compared to oral administration of Neoral®. Moreover, CsA levels in blood, liver and kidney were much lower following topical administration. Thus, the results confirmed that topical administration was an effective means to increase CsA levels in the skin while decreasing systemic exposure.

Despite the strong pharmacological rationale for its use, clinical studies have shown that psoriasis patients display considerable variability in their response to CsA [6,7]. Hirano et al. [6] measured the CsA concentration that gave 50% inhibition (IC_{50}) of mitogen-stimulated peripheral blood mononuclear cells (PBMC) proliferation in 33 psoriasis patients. They observed that the IC_{50} ranged from 0.1 to 120.6 ng/ml and divided the population into two groups—good and poor responders (51.5% and 48.5% of the population, respectively). Umezawa et al. [7] subsequently showed that more hepatopathies and nephropathies were reported in psoriatic patients with low sensitivity to CsA since these patients obviously required higher systemically administered doses. Therefore, in order to avoid unnecessary systemic exposure, a targeted and effective topical therapy would be preferable to oral administration of CsA.

However, efficient delivery of poorly water soluble drugs such as CsA into the stratum corneum is a considerable challenge since formulation excipients used to solubilise the drug frequently reduce thermodynamic activity. In addition to physicochemical considerations, physiological factors must also be taken into account—psoriatic lesions can have thickened stratum corneum and epidermis. Moreover, from a patient compliance perspective, topical formulations should ideally have a once-daily (or even lower) application frequency, be easy to apply, have quick absorption and absence of greasiness [2].

Numerous efforts have been made to improve topical delivery of CsA into skin with a strong emphasis on the development of colloidal nanostructured vehicles including microemulsions [5,8,9], monoolein liquid crystalline formulations [10,11], amphiphilic gels [12] and solid lipid nanoparticles [13]. The challenge is to increase cutaneous bioavailability without producing a concomitant increase in transdermal permeation and, hence, systemic exposure *in vivo*.

The objective of the present study was to investigate the incorporation of CsA into polymeric micelles and so develop simple, single component aqueous formulations for topical delivery into skin to treat psoriasis. Micelles are colloidal systems usually composed of amphiphilic molecules, able to self-assemble above the critical micelle concentration (CMC). These spherical structures possess a hydrophilic shell and a hydrophobic core. In the case of polymeric micelles, the amphiphilic compound is a block copolymer with lipophilic/hydrophilic component blocks. Trimaille et al. [14] developed a methoxy-poly(ethylene glycol)-poly(hexylsubstituted lactides) (MPEG-hexPLA) diblock copolymer: the methoxy-poly(ethylene glycol) chain provided the hydrophilic "head", whereas the lipophilic "tail" came from the hexyl substituted polylactide component. The presence of hexyl groups resulted in an increased lipophilicity of the core and a low CMC (1.6×10^{-6} M) compared to the standard MPEG-PLA [14] facilitating the incorporation of highly lipophilic drugs. CsA-loaded MPEG-dihexPLA micelles (dihexyl substituted derivative) were first developed and tested for parenteral use [15]. It was shown that micelles produced a significant increase in CsA water solubility and that the formulations were stable for up to 1 year at 4 °C. After a forced degradation, the copolymer formed two non-toxic compounds: 2-hydroxyoctanoic acid and PEG [16]. Moreover, no toxicity was demonstrated *in vitro* in various cell lines and *in vivo* using chick embryo chorioallantoic membrane (CAM) model for both the copolymer only and polymeric micelles up to copolymer concentrations of 20 mg/ml [15].

Ocular administration of CsA using MPEG-dihexPLA micelles also showed promising results [17,18]. However, skin and cornea possess very different histological structures and different barrier properties; therefore, the ability of MPEG-dihexPLA micelles to deliver CsA into the skin must be determined experimentally and this was the objective of the first part of the present study. The second part involved an investigation into the cutaneous localisation of the drug and the micelles and a visualisation of transport routes in the skin. Confocal laser scanning microscopy (CLSM) studies are very useful to achieve this goal. Small, low molecular weight dyes are generally employed as "model drugs" but it is not always possible to accurately replicate the properties of the drug of interest. Furthermore, these "model drugs" are inappropriate in our case as both the copolymer and incorporated drug are of higher molecular weight. Therefore, in order to investigate the localisation of the copolymer and CsA in skin using CLSM, both were chemically coupled to fluorescent dyes—Nile Red and fluorescein, respectively.

2. Materials and methods

2.1. Materials

Ciclosporin A was purchased from Hangzhou Dayangchem (Hangzhou Zhejiang, PR China). The novel amphiphilic MPEG-dihexPLA copolymer (methoxy-poly(ethylene glycol) di-(hexyl-substituted polylactide)) and its Nile Red labelled analogue were synthesised in-house as described previously [14,19]. Their respective structures are presented in Fig. 1. The MPEG-dihexPLA copolymer had a Mn of 6080 g/mol and a polydispersity index (P.I.) of 1.15 according to GPC measurements (the GPC setup consisted of a Waters Styragel HR1-4 column, Waters 717 autosampler, Waters 515 HPLC pump and a Waters 410 differential refractometer (Waters; Baden-Dättwil, Switzerland)). The analysis was carried out using polystyrene (PS) with different molecular weights as calibration standards (PSS; Mainz, Germany).

The starting materials, 4-vinylaminobenzene, and Boc-anhydride (di-tert-butyldicarbonate) used to synthesise Fluo-CsA were purchased from TCI Europe (Eschborn, Germany) and Fluka (Buchs, Switzerland), respectively. The second generation Grubbs catalyst, trifluoroacetic

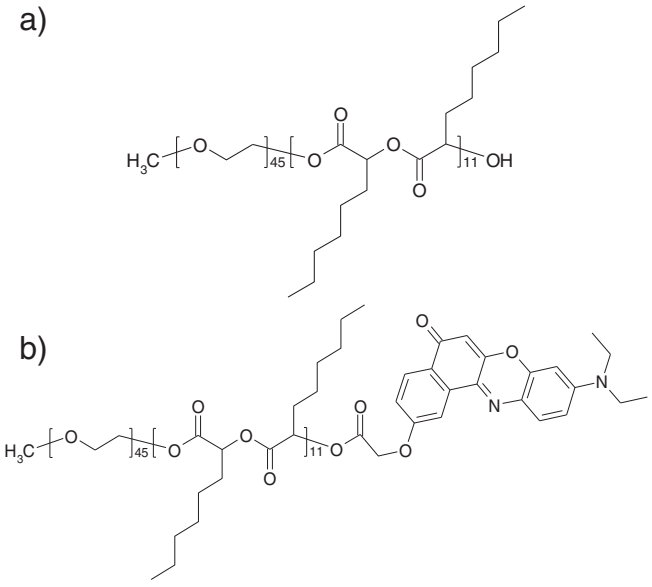

Fig. 1. a) Structure of MPEG-dihexPLA copolymer and b) structure of Nile Red labelled MPEG-dihexPLA copolymer.

acid, tetrahydrofuran, octanol, acetone, tetrabutylammonium hydrogen sulphate (TBAHS), acetic acid, formic acid, hydrochloric acid, citric acid and sodium chloride were supplied by Sigma-Aldrich (Steinheim, Germany). NHS-fluorescein was purchased from Thermo Scientific (Dreieich, Germany). Silica gel (SiliaFlash P60 with a particle size of 40–63 μm) was bought from Parc-Technologique BLVD (Quebec City, Canada). Sodium hydroxide solution (40 M), potassium chloride and sodium hydrogen phosphate were obtained from Fluka (Buchs, Switzerland). Triethylamine (TEA), potassium dihydrogen phosphate and potassium hydrogen phosphate were supplied by Acros Organics (Geel, Belgium) and propylene glycol by Hänseler AG (Herisau, Switzerland). Bovine serum albumin (BSA) was purchased from Axon Lab (Baden-Dättwil, Switzerland). All other solvents (methanol, n-hexane, ethyl acetate, dichloromethane, chloroform, acetonitrile (MeCN)) were HPLC grade (HiPerSolv Chromatonorm: Darmstadt, Germany). Ultra-pure water (Millipore Milli-Q Gard 1 Purification Pack resistivity > 18MΩcm; Zug, Switzerland) was used to prepare all solutions.

2.2. Synthesis and characterisation of a fluorescent analogue of ciclosporin A (Fluo-CsA)

2.2.1. Synthesis of a fluorescent analogue of ciclosporin A (Fluo-CsA)

CsA was labelled with the fluorescent dye, NHS-fluorescein, using 4-vinylbenzylamine (4-VB) as a linker using a four-step procedure, adapted from Gaali et al. [20]. An overview of the four steps is shown in Fig. 2. The primary amine of 4-VB (①) was first Boc-protected (②) and then attached to CsA (③) by a cross-metathesis catalysed by the Grubbs second generation catalyst to yield (④), which was then deprotected and labelled with the fluorescent dye, NHS-fluorescein (⑥) to produce the final fluorescent analogue of CsA: Fluo-CsA (⑦).

The detailed methods used during the different steps are described in the Supplementary Data. In order to confirm the success of the different reaction steps, the intermediate products were analysed by mass spectroscopy (API 150EX, AB Sciex; Framingham, USA) and NMR (Varian Gemini 300 BB, 300 MHz, Varian; Palo Alto, USA). $CDCl_3$ or DMSO-d_6 were used as solvents (Supplementary Data). The final product, Fluo-CsA, was characterised by high resolution mass spectroscopy and its purity was tested consecutively by HPLC, the product appeared to be 98% pure. The total yield of the four reaction steps was 61%.

2.2.2. Structural comparison of CsA and Fluo-CsA

In order to examine the possible conformational changes of CsA when compared to Fluo-CsA, a structural analysis was performed by using computational methods. The analysis was carried out using the Maestro programme, a tool from the Schrödinger 2013 package (Maestro; Schrödinger, LLC: Portland, OR, 2009). Energy minimisations were carried out in water by applying 10,000 iterations with a conjugated gradient of 0.05 kcal/mol and using the OPLS-2005 force-field.

CsA was used as the reference structure [PDB code: 1CYA]. As fluorescein carries ionisable groups, Fluo-CsA was submitted to the minimisation steps considering both of its protonation states: neutral and deprotonated. The conformation of the backbone of the compounds was investigated. The structures were represented using the VMD program [21]. Finally, the lipophilicity potential surface of the CsA and Fluo-CsA was analysed using Sybyl 2.1.1 programme (SYBYL-X 2.1.1, Tripos International, St. Louis, Missouri, USA).

2.2.3. Determination of the distribution coefficient of CsA and Fluo-CsA

The distribution coefficients (log D) of Fluo-CsA and CsA were determined experimentally using the shake flask method in order to compare their lipophilicity as a function of pH (4–8) [22]. Solutions of each compound (100 μg/ml) were prepared in octanol (organic phase). Buffer solutions (pH 4–8) constituted the aqueous phase. Buffer solutions were saturated with octanol and vice versa for 24 h prior to measurement. For the experiment, glass vials were filled with 1 ml of buffer solution and 0.5 ml of drug-in-octanol solution. The two immiscible phases were stirred for 24 h at RT. Finally, CsA and Fluo-CsA were quantified in the octanol phase after appropriate dilution. The concentration in the aqueous phase was subsequently determined and log D as a function of pH calculated according to Eq. (1).

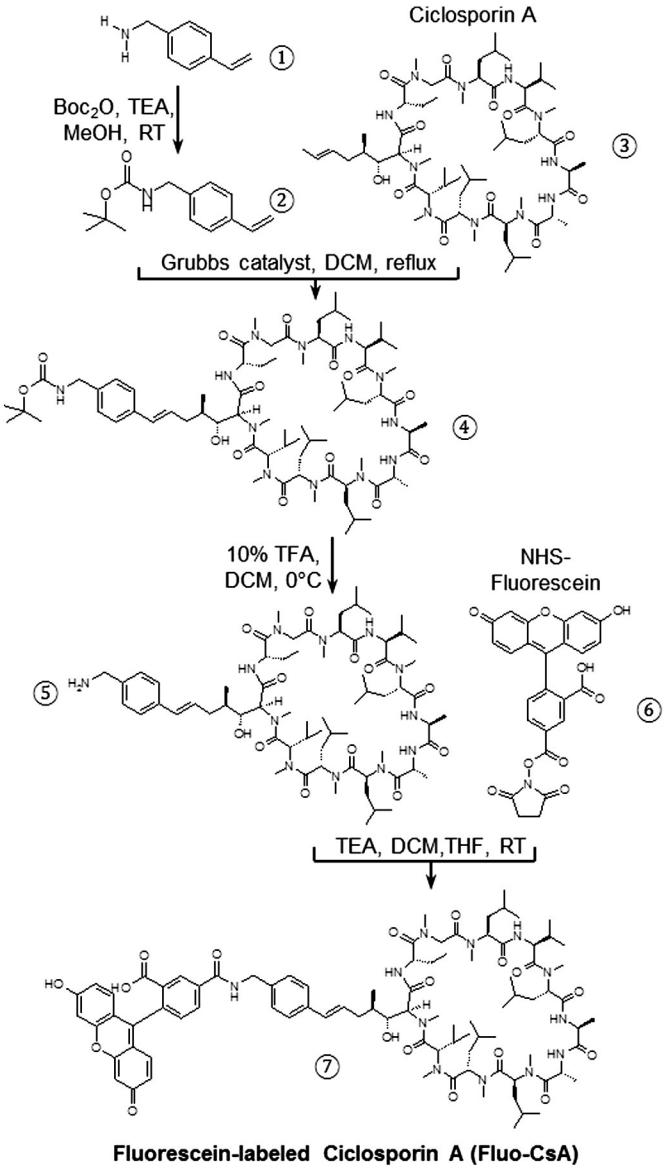

Fig. 2. Synthesis of fluorescein-labelled CsA (Fluo-CsA, ⑦).

$$\mathrm{Log\,D_{octanol/buffer\ pH\ x}} = \mathrm{Log}\left(\frac{[\text{CsA or Fluo-CsA}]\text{octanol}}{[\text{CsA or Fluo-CsA}]\text{buffer pHx}}\right) \quad (1)$$

2.3. Analytical methods

Both CsA and Fluo-CsA were quantified using high performance liquid chromatography (HPLC). The HPLC system consisted of a P680 HPLC pump, an ASI-100 automated sample injector and a TCC-100 thermostatted column compartment and UV and fluorescent detectors, UVD170U/RF 2000, respectively (formerly Dionex AG, now Thermo Fisher Scientific AG; Reinach, Switzerland).

2.3.1. Quantification of CsA

For the quantification of CsA, a reverse phase column (Lichrospher 100, RP 18, 125*4.0 mm, 5 μm) was thermostated at 40 °C. The mobile phase consisted of a mixture of MeCN:phosphoric acid 0.1% buffer, pH 3 (75:25) at a flow rate of 1 ml/min. CsA was detected by its UV absorbance at 230 nm. All standards and samples were prepared in acetonitrile. The retention time of CsA was 6.2 min and the method was validated (Supplementary Data) according to ICH and FDA guidelines [23,24]. The limits of detection (LOD) and quantification (LOQ) were 0.57 and 1.72 μg/ml respectively.

2.3.2. Quantification of Fluo-CsA

Quantification and purity testing of the newly synthesised compound were performed using a Jupiter 5 μm, C4, 300 Å 150 × 4.60 mm column heated at 30 °C. The mobile phase, comprised a 70:30 mixture of MeOH:pH 8 buffer (5 mM K_2HPO_4, 5 mM TBAHS) and the flow rate was 1 ml/min. The excitation and emission wavelengths of the fluorescence detector were set at 490 nm and 514 nm, respectively. The method was validated (Supplementary Data) according to ICH and FDA guidelines [23,24]. The LOD and LOQ were 0.11 and 0.35 μg/ml, respectively.

2.4. Micelle preparation

2.4.1. Preparation of CsA loaded micelles

Micelles were prepared using the solvent evaporation method [25,26]. Briefly, CsA (8–32 mg) and the copolymer (20–80 mg) were dissolved in 2 ml of acetone. This organic solution was then added dropwise under sonication (Branson digital Sonifier® S-450D; Carouge, Switzerland) into 4 ml of ultra-pure water. Acetone was then evaporated with a rotary evaporator (Büchi RE 121 Rotavapor; Flawil, Switzerland). The final copolymer concentration ranged from 5 to 20 mg/ml. After equilibration overnight, the micelle solution was centrifuged at 10,000 rpm for 15 min (Eppendorf Centrifuge 5804; Hamburg, Germany) to remove non-incorporated drug and the supernatant was collected.

2.4.2. Preparation of Fluo-CsA loaded micelles

In the case of Fluo-CsA loaded micelles, the copolymer mixture consisted of MPEG-dihexPLA and the fluorescent NR-MPEG-dihexPLA copolymers (7:3) in 2 ml of acetone. Fluo-CsA (6.5 mg) was added to this mixture. The micelles were prepared using the solvent evaporation method described above. The final copolymer concentration was 5 mg/ml.

2.5. Micelle formulation characterisation

2.5.1. Size determination

The hydrodynamic diameter (Z_{av}), polydispersity index (P.I.), volume-weighted and number-weighted diameter (d_v and d_n) of micelles were measured using dynamic light scattering (DLS) with a Zetasizer HS 3000 (Malvern Instruments Ltd.; Malvern, UK). Parameters were obtained after three runs of ten measurements at an angle of 90° and a temperature of 25 °C.

2.5.2. Morphology determination

Micelle morphology was characterised with transmission electron microscopy (TEM) (Technai G2 20) using the negative staining method. 5 μl of the micelle solution was applied onto an ionised carbon-coated 200 mesh copper grid (0.3 Torr, 400 V for 20 s). The grid was then deposited for 1 s onto a 100 μl drop of a saturated uranyl acetate aqueous solution and then onto a second 100 μl drop for 30 s. Excess staining solution was removed and the grid was dried at room temperature prior to insertion into the sample holder and TEM analysis. TEM images were processed using Image J software (Image J 1.45 s).

2.6. Micelle CsA and Fluo-CsA content determination

CsA or Fluo-CsA loading in the micelles was quantified as described above (2.3.1 and 2.3.2, respectively). To ensure complete micelle destruction and release of the incorporated substance, 1:20, 1:50 1:100 dilutions were made for each formulation in either acetonitrile or methanol for CsA or Fluo-CsA loaded micelles, respectively. The drug content, drug loading and incorporation efficiency were calculated using Eqs. (2)-(4), respectively:

$$\text{Drug content (mg drug/ ml formulation)} = \frac{\text{mass of drug in the formulation (mg)}}{\text{Volume of the formulation (ml)}} \quad (2)$$

$$\text{Drug loading (mg drug/g copolymer)} = \frac{\text{[drug]in the formulation (mg/ml)}}{\text{[Copolymer]in the formulation (g/ml)}} \quad (3)$$

$$\text{Incorporation efficiency (\%)} = \frac{\text{mass of drug incorporated into micelles (mg)}}{\text{mass of drug introduced (mg)}} \times 100 \quad (4)$$

2.7. Skin preparation

Porcine ear skin was used for the *in vitro* skin transport studies [27–29]. Ears were purchased from a local abattoir (CARRE, Rolle, Switzerland). After washing under running cold water, skin samples with a thickness of ≈0.75 mm were harvested using a Zimmer® air dermatome (Münsingen, Switzerland). Hairs were excised from the skin surface using clippers. Discs with a diameter of 32 mm, corresponding to the formulation application area, were punched out using a puncher (Berg & Schmid HK 500, Urdorf, Switzerland) Skin samples were frozen at −20 °C for a maximum period of 3 months. Prior to the experiment, skin samples were thawed at room temperature and placed for 15 min in 0.9% saline solution for rehydration.

Human skin samples were collected immediately after surgery from the Department of Plastic, Aesthetic and Reconstructive Surgery, Geneva University Hospital (Geneva, Switzerland). The study was approved by the Central Committee for Ethics in Research (CER: 08-150 (NAC08-051); Geneva University Hospital). Hypodermis and fatty tissue were removed and discs corresponding to the permeation area were punched out (Berg & Schmid HK 500; Urdorf, Switzerland). The skin discs (again with a diameter of 32 mm) were subsequently horizontally sliced with a Thomas Stadie-Riggs slicer (Thomas Scientific; Swedesboro, NJ, USA) to obtain a thickness of ~0.8 mm. The skin was stored in a biobank at −20 °C for a maximum period of 3 months.

2.8. In vitro delivery experiments

Skin samples were mounted in standard Franz diffusion cells (area = 2 cm^2, Milian; Meyrin Switzerland). 500 mg of micelle formulation or control were added to the donor compartment. The receptor compartment (PBS pH 7.4 + 1% BSA, 10 ml) was stirred at 250 rpm at room temperature during 1, 4, 8, 12 or 24 h. At the end of the experiment, 1 ml of receptor phase was withdrawn to quantify permeation of CsA. After centrifugation at 10,000 rpm for 15 min permeation samples were analysed by HPLC. The diffusion cells were subsequently dismantled and the skin samples were carefully washed for 5 s under running water to remove the residual formulation from the stratum corneum surface. The wash procedure was validated (Supplementary Data). Skin samples were then cut into small pieces and deposited CsA was extracted by soaking the skin in 4 ml of acetonitrile or methanol, respectively, for 4 h with continuous stirring at room temperature.

The extraction samples were centrifuged at 10 000 rpm for 15 min and quantified by HPLC. The extraction procedure was also validated (Supplementary Data).

2.9. Data analysis

Data were expressed as the mean ± SD. Outliers determined using the *Dixon test* were discarded. Results were evaluated statistically using either analysis of variance (ANOVA) or analysis of means by *Student's t-test*. *Student–Newman–Keuls test* was used when necessary as *post-hoc* procedure. The level of significance was fixed at $\alpha = 0.05$.

2.10. Visualisation of micelle penetration pathways using Fluo-CsA loaded micelles

Upon completion of skin delivery experiments with fluorescent micelles, the skin samples were cut in longitudinal sections. Each individual sample was then placed on a glass slide with the exposed cross-section (epidermis to dermis) facing the objective. Visualisation of delivery pathways was investigated by confocal laser scanning microscopy (CLSM) (LSM 710, Zeiss, Germany). The excitation wavelengths, fluorescence emission wavelengths, laser power, pinhole and master gain for each dye are presented in Table 1.

The confocal images were obtained with an air Achroplan 20× objective and acquired using Zen software (Carl Zeiss, Germany). To ensure accurate comparison, all samples were visualised using the same parameters. CLSM pictures were finally processed using Image J software (Image J 1.45 s).

3. Results and discussion

3.1. Structural comparison of CsA and Fluo-CsA

The minimized structures and the lipophilicity surface potential of CsA and Fluo-CsA in its different protonation states are presented in Fig. 3.

As shown in Fig. 3a, the superimposition of the three minimised structures reveals no significant conformational differences between Fluo-CsA and CsA. This observation is also supported by the root-mean-square deviation of atomic positions (RMSD) values, which have been calculated among the three structures (Table 2).

It should also be noted that the attachment of the fluorescent dye did not induce any significant change in the lipophilicity potential surface of CsA (Fig. 3b). Therefore, it can be concluded that the fluorescently labelled CsA is conformationally very similar to native CsA and may be used as a representative model.

3.2. CsA and Fluo-CsA log D determination

Although the computational studies predicted that Fluo-CsA was conformationally similar to native CsA and that it had similar lipophilicity, this needed to be confirmed experimentally at the macroscopic level. Therefore, the distribution coefficients (log D) of both compounds were determined from pH 4 to pH 8. The log D of both compounds was between 1.81 ± 0.26 and 2.08 ± 0.11 over the tested pH range (Fig. 4). These results were similar to the literature data which indicated a log D of 2.73 for CsA independent of pH [30].

No significant difference (*t-test*: $p < 0.05$) was found between the log D of CsA and Fluo-CsA from pH 4 to 7. However, at pH 8, the log D of Fluo-CsA was significantly lower (1.68 ± 0.02 vs. 2.08 ± 0.11). Although this may have been a statistical anomaly, fluorescein has multiple ionisable groups [31]. In strongly acidic conditions it exists as a neutral compound, increasing pH results in deprotonation of the carboxylic acid moiety to yield the mono-anion and finally in weakly acidic conditions, the phenol is deprotonated (pKa ~6.4) to produce the di-anion (Fig. 4). Therefore, at pH 8, the fluorescein moiety of Fluo-CsA carries a double negative charge and this tends to render the compound more hydrophilic, lowering its log D. However, given that the skin surface pH is ~5.0–5.5, that the micelle formulation pH was 5.5–6 and that, in general, topical formulations usually have a pH ranging from weakly acidic to neutral [32], the results indicate that chemical modification of CsA and the addition of ionisable groups did not significantly affect its partition properties over the relevant pH range. Therefore, from a physicochemical point of view, the synthesised fluorescent analogue of CsA was considered to be a suitable model for subsequent CLSM visualisation studies.

3.3. Micelle preparation and characterisation

3.3.1. CsA loaded micelles

Micelles of various copolymer contents (from 5 to 20 mg/ml of copolymer) were formulated and characterised (Table 3).

CsA content increased linearly with increasing copolymer content ($y = 0.292x + 0.3108$; $R^2 = 0.9991$). CsA loading remained fairly constant with values comprised between 310.93 ± 9.36 and 333.75 ± 5.56 mg_{CsA}/g_{copo}. The highest drug loading 333.75 ± 5.56 mg_{CsA}/g_{copo} was achieved in Formulation A, which had the lowest copolymer content (5 mg/ml). Formulation D (with 20 mg/ml of copolymer) was able to incorporate 311.23 ± 1.16 $mg_{CsA}/g_{copo,}$ leading to a maximal CsA content of 6.225 ± 0.223 mg/ml. Considering that the aqueous solubility of CsA is only 0.012 mg/ml [15], the micelles were able to increase this by up to 518-fold.

All micelles were found to have an average hydrodynamic diameter, Z_{av}, between 25 and 52 nm, and a P.I. between 0.238 and 0.699. The size of the micelles and P.I. increased slightly with copolymer content, indicating that some aggregation might occur at high copolymer contents. TEM observations (Fig. 5) showed that CsA micelles with low copolymer content (5 mg/ml; Fig. 5a) were mainly spherical with diameters ranging from 15 to 40 nm, whereas formulations with higher copolymer content (20 mg/ml; Fig. 5b) showed still small, yet slightly elongated worm-like micelles. This last observation could explain the high Zav and P.I. determined by DLS for this formulation. However, overall results indicated that polymeric micelle nanocarriers with a high CsA loading and homogeneous size could be formulated.

3.3.2. Fluo-CsA loaded micelles

Fluorescent NR-MPEG-dihexPLA micelles (5 mg/ml of copolymer) were loaded with Fluo-CsA. A loading of 324.79 ± 4.2 $mg_{Fluo\text{-}CsA}/g_{copo}$ was achieved. The Fluo-CsA content of the formulation was 1.62 ± 0.03 mg $_{Fluo\text{-}CsA}$/ml formulation. These results are comparable to the corresponding values for CsA micelles (333.75 ± 5.56 mg_{CsA}/g_{copo} and 1.669 ± 0.027 mg/ml, respectively). Fluo-CsA loaded micelles were found to have an average hydrodynamic diameter Z_{av} of 27 nm, a P.I. of 0.328. TEM observations (Fig. 5c) showed that the micelles were spherical with sizes ranging from 19 to 45 nm.

These results indicated that similar amounts of CsA and the fluorescent analogue (Fluo-CsA) were incorporated into the micelles. Furthermore, fluorescent micelles presented similar sizes and morphology to

Table 1
Settings used for CLSM.

Dye	Excitation	Emission	Laser power (%)	Pinhole (μm)	Master gain
Nile Red	HeNe diode laser at 543 nm	607–674 nm	15	91	800
Fluo-CsA	Ar laser at 488 nm	504–530 nm	20	100	750

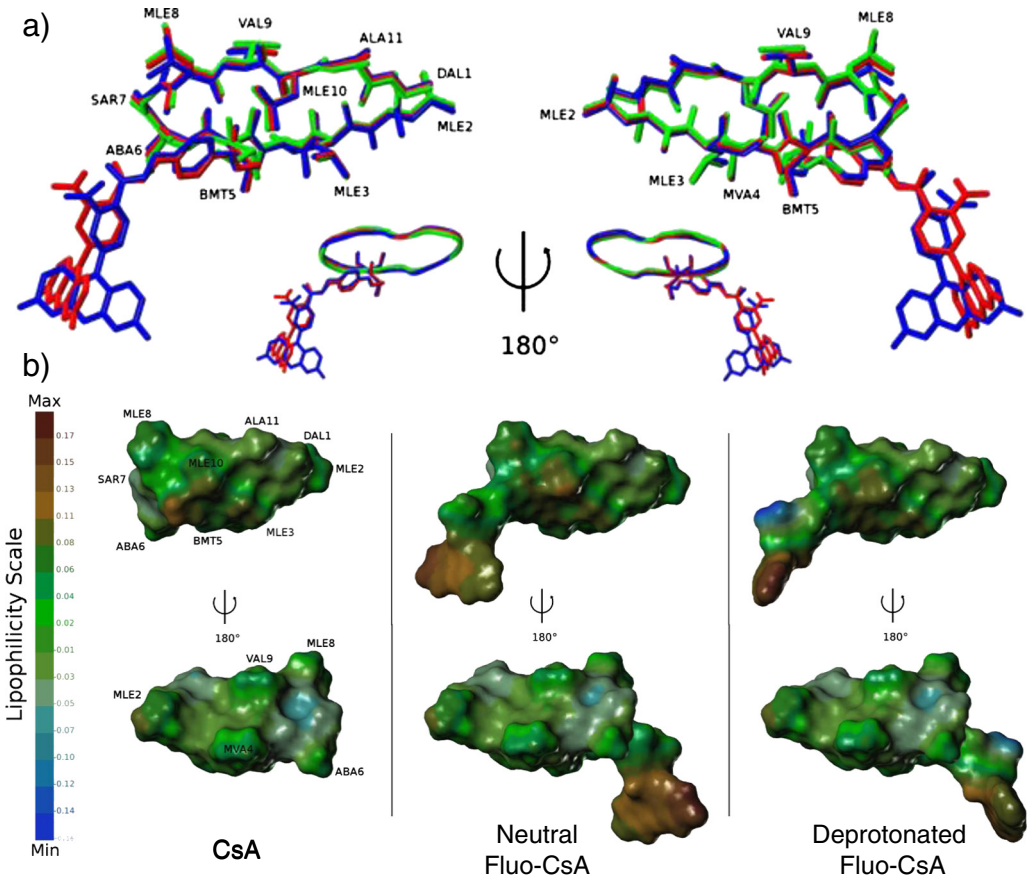

Fig. 3. a) Superimposition of CsA and Fluo-CsA structures in its two distinct protonation states. CsA is coloured green, the neutral and the deprotonated states of Fluo-CsA are respectively in blue and in red, b) lipophilicity potential surface of CsA, neutral and deprotonated states of Fluo-CsA, respectively. The lipophilicity scale ranges from brown (most lipophilic) to blue (most hydrophilic surface). The minimum/maximum lipophilicity values for the different structures are: CsA (−0.083, 0.113), neutral Fluo-CsA (−0.072, 0.100) and deprotonated Fluo-CsA (−0.169, −0.095). The decreased lipophlicity of deprotonated Fluo-CsA reflects the impact of the ionised carboxylate moiety.

the CsA loaded micelles. Thus, Nile Red labelling of the copolymer did not affect the micelle size. As a result, NR-MPEG-dihexPLA micelles loaded with Fluo-CsA were considered to be an accurate model to investigate the skin penetration pathways of both the drug and polymeric micelles.

3.4. In vitro delivery experiments

3.4.1. Influence of CsA content in micelle formulation on skin delivery

CsA permeation across porcine skin after application of the formulations for 24 h was undetectable by the HPLC-UV method, suggesting that drug permeation was extremely low and that *in vivo*, only very small amounts might reach the systemic circulation, which is primordial when the disease is limited to skin. The increase in copolymer content (5 to 20 mg/ml), and subsequently in CsA content (1.669 ± 0.027 to 6.225 ± 0.223 mg/ml), resulted in an increased topical delivery of CsA into the skin ranging from 7.4 ± 1.1 to 16.3 ± 3.0 μg/cm^2 and delivery efficiencies ranging from 1.00 ± 0.27 to 1.78 ± 0.27% (Fig. 6a). CsA delivery from the control formulation (6.2 mg/ml solution in propylene glycol) was 18-fold lower than that from the micelle formulation (0.9 ± 0.5 and 16.3 ± 3.0 μg/cm^2, respectively) at equivalent CsA content. Although few studies have been conducted using polymeric micelles as skin drug delivery systems, several hypotheses have been proposed to describe the possible interactions between micelles and skin. It has been suggested that intact micelles might permeate through intact skin [33], but this is unlikely, given the high molecular weight of the polymers used for micelle formation. Other studies suggest that the enhancement can be due to micelle disassembly when in contact with skin and action of individual polymer chains as chemical penetration

Table 2
RMSD values (Å) among the backbone atoms of CsA and Fluo-CsA in its different protonation states.

	CsA	Neutral Fluo-CsA	Deprotonated Fluo-CsA
CsA	–	0.33	0.20
Neutral Fluo-CsA	0.33	–	0.14
Deprotonated Fluo-CsA	0.20	0.14	–

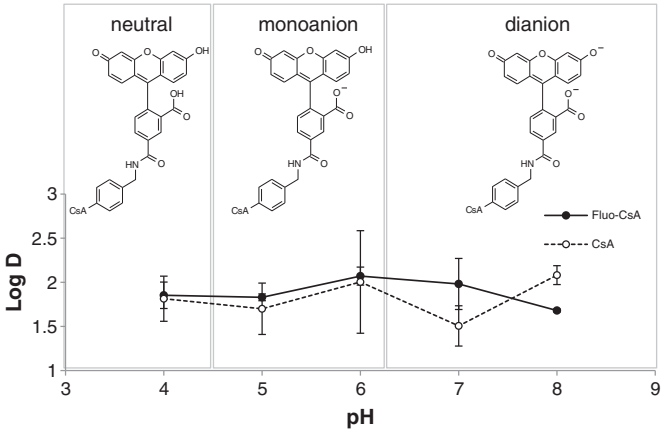

Fig. 4. Comparison of Fluo-CsA and CsA Log D as a function of pH (data are expressed as mean ± SD; n = 3).

Table 3
Micelle formulation characterisation in terms of drug incorporation and size (data are expressed as mean ± SD; n = 3).

Formulation	Copolymer content (mg/ml)	TARGET drug loading (mg_{CsA}/g_{copo})	CsA content characterisation			Size characterisation			
			Drug loading ± SD (mg_{CsA}/g_{copo})	Drug content ± SD (mg_{CsA}/ml)	Incorporation efficiency ± SD (%)	Zav (nm)	P.I.	d_n (nm) [%]d_n	d_v (nm) [%]d_v
A	5	400	333.75 ± 5.56	1.669 ± 0.027	83.44 ± 1.39	28	0.238	19 [100.0%]	13 [100.0%]
B	10	400	327.28 ± 9.26	3.273 ± 0.093	81.82 ± 2.31	25	0.164	19 [100.0%]	15 [98.3%]
C	15	400	310.93 ± 9.36	4.664 ± 0.140	77.73 ± 2.34	41	0.498	20 [100.0%]	16 [100.0%]
D	20	400	311.23 ± 1.16	6.225 ± 0.223	77.81 ± 2.79	52	0.699	21 [98.9%]	17 [100.0%]
Fluorescent micelles	5	400	324.79 ± 4.2	1.626 ± 0.030	81. 91 ± 1.05	27	0.328	15 [100.0%]	13 [100.0%]

enhancers [34]. Superior delivery of econazole nitrate from MPEG-dihexPLA micelles as compared to a marketed liposomal formulation was attributed to the small size of the carriers, increased skin contact area and depot formation at the skin surface or in appendages [26].

Micelles in a formulation applied to the skin, will be subject to random Brownian motion in the solution. Some will reach the skin surface and given the number of CsA molecules present per micelle, this results in high local concentrations/thermodynamic activity which favours partitioning into the stratum corneum. Although CsA molecules present in the control propylene glycol formulation will also enter into contact with the surface through Brownian motion, the local concentrations are lower and hence there may be a lower thermodynamic driving force to partition. Of course, this does not preclude interactions between copolymer and the upper layers of the stratum corneum that perturb lipid organisation/barrier function and so facilitate delivery.

The presence of a linear relationship between CsA delivery and CsA content in the micelle formulations ($y = 2.7345x - 0.2486$; $R^2 = 0.9588$) (Fig. 6b) suggested that the increase in CsA content in the formulations was due to the increase in copolymer content, i.e. to an increased number of micelles having an essentially constant drug loading (from 333.75 ± 5.56 to 311.23 ± 1.16 mg_{CsA}/g_{copo}; Table 3). As argued above, the increased number of micelles would provide better skin coverage and increase delivery as compared to the propylene glycol formulation despite its high drug content (equivalent to that of the 20 mg/ml copolymer formulation).

It was observed that delivery from the 5 mg/ml copolymer formulation was higher (1.78 ± 0.27% of the applied dose) than that predicted by the linear model. It should be mentioned that the 5 mg/ml copolymer formulation had a higher drug loading than the other micelle formulations (Table 3), resulting in a higher thermodynamic activity of the drug inside the micelle core. Therefore, although fewer micelles were in contact with skin, the increased thermodynamic driving force, i.e. the tendency of the drug to "escape" from the micelle was high and overall delivery was increased and was similar to that of the 10 mg/ml copolymer formulation.

From these results it was possible to conclude that CsA delivery from the micelle formulations into the skin could be fine-tuned by modulating either the copolymer content or the drug loading. The 5 mg/ml copolymer formulation was selected for further experiments as it seemed to be optimal in terms of thermodynamic activity and presented good size and morphology characteristics.

3.4.2. Kinetics of CsA skin deposition and validation in human skin

The 5 mg/ml formulation was selected to study the kinetics of CsA skin deposition over 24 h (Fig. 7a). CsA skin deposition was 1.1 ± 0.5 μg/cm^2 after 1 h and increased before reaching a plateau between 12 h and 24 h (8.7 ± 1.8 and 7.4 ± 1.1 μg/cm^2 respectively). Similar behaviour was previously observed with flufenamic acid [35] and described using a Michaelis–Menten model:

$$CsA_{dep}\left(t_{app}\right) = \frac{CsA_{dep,\,max} \times t_{app}}{t_{max/2} + t_{app}} \quad (5)$$

where CsA_{dep} (t_{app}) and $CsA_{dep,max}$ describe the deposition of CsA as a function of formulation application time (t_{app}) and the maximum (plateau) value and $t_{max/2}$ is that time at CsA_{dep} reaches half of the maximum value. It was hypothesised that there were a limited number of available molecular binding sites and hence the process was saturable. Fitting of the data ($R^2 = 0.7434$) to Eq. (5) as shown in Fig. 7a gave $CsA_{dep,max}$ and $t_{max/2}$ values of 10.6 μg/cm^2 and 6.8 h, respectively.

As mentioned above, psoriatic patients possess high variability in terms of their sensitivity to CsA. For example, in a psoriatic patient with very low CsA sensitivity, the IC_{50} was 120.6 ng/ml and IC_{90} was 1000 ng/ml [6]. When applied to our *in vitro* model, this IC_{90} corresponds to a minimum drug content in skin of 1 μg per cm^3 of tissue. The micelle formulation with the lowest copolymer and drug content resulted in a CsA skin concentrations of 14.6 ± 6.6 μg/cm^3 after only 1 h of application and 98.6 ± 14.6 μg/cm^3 after 24 h, which exceeds the IC_{90} in poor responders by 15- and 99-fold, respectively. When applied to human skin for 1 h, the MPEG-dihexPLA micelle formulation yielded a statistically similar CsA delivery of 1.4 ± 0.6 μg/cm^2 (Fig. 7b), suggesting that supra-therapeutic levels in human skin could be achieved after a short 1 h application time. Nevertheless, a validation in diseased human skin is necessary as the barrier function in psoriatic skin can be highly modified [2].

Several colloidal formulations including microemulsions [5,8,9], monoolein liquid crystalline formulations [10,11], amphiphilic gels [12] and solid lipid nanoparticles [13] have been developed in order to increase skin topical bioavailability of CsA. However, only studies conducted by Lopes et al. [10,11,36] were performed using porcine skin and thus are relevant for comparison with the data from the present study.

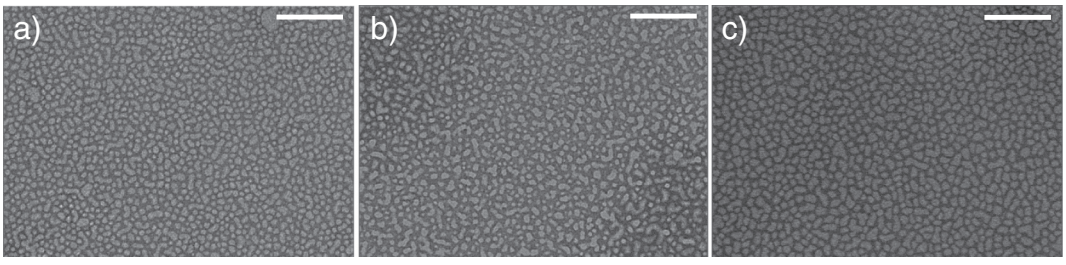

Fig. 5. TEM pictures of a) CsA loaded micelles with 5 mg/ml copolymer content, b) CsA loaded micelles with 20 mg/ml copolymer content and c) Fluo-CsA loaded fluorescent micelles with 5 mg/ml copolymer content. Bar = 200 nm.

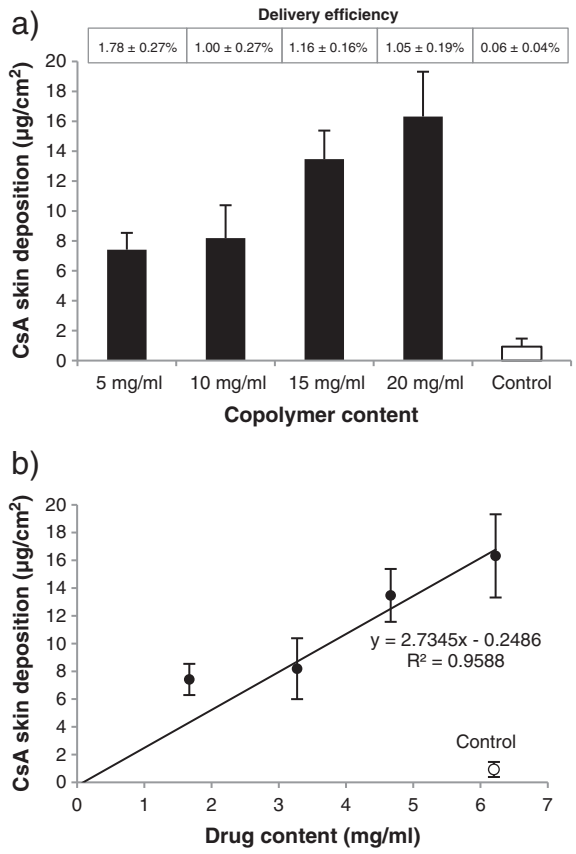

Fig. 6. CsA skin deposition from CsA-loaded micelles as a function of a) copolymer content and b) CsA content. A 6.2 mg/ml CsA solution in propylene glycol served as control (data are expressed as mean ± SD; n = 6). The delivery efficiencies (dose delivered/dose applied) are presented in % in a).

CsA deposition after 12 h from a formulation containing 10% monoolein (MO) in propylene glycol (PG) exceeded 100 µg/cm^2 [36]. Although much higher than that obtained with the micelle formulations described here, the differences can be explained by the high CsA content in the formulation (4%) and the presence of ethanol, a known penetration enhancer, in the receptor solution (10%). The latter may have increased skin permeability by diffusing into the tissue from the dermis as evidenced by the presence of CsA in the receiver compartment. MO can form various liquid crystalline structures when mixed with water [37] and in a subsequent study, MO reverse hexagonal and cubic phases were formulated [10] by the addition of 5% oleic acid to the cubic phase. Skin delivery of CsA from cubic and hexagonal phase formulations was approximately 210 µg/cm^2 and 79 µg/cm^2, respectively; however, some permeation was again observed. It is difficult to conclude whether these liquid crystalline formulations are superior to MPEG dihex-PLA micelles given the greater CsA content (4%), different experimental conditions (inclusion of 10% ethanol in the receiver phase) and the presence of oleic acid.

In another study, water rich hexagonal nano-dispersions of MO and oleic acid (2% w/w) were formulated with a CsA content of 0.6% [11]. The nanoparticulate nature of this formulation and its CsA content were closer to that of the micelle formulations used in the present study and allowed a more accurate comparison. *In vitro* topical skin delivery of CsA from hexagonal nano-dispersions was approximately 61 µg/cm^2 after application for 12 h, which is higher than that yielded by the micelles. However, the ethanol content in the receptor solution (10%) should again be emphasised. The penetration enhancing activity of MO and oleic acid is due to their linear lipidic structures and to their low molecular weight (356.54 g/mol and 282.46 g/mol for MO and oleic acid, respectively) allowing them to interact with stratum corneum lipids, disrupt their organisation and so improve transport. In contrast to the MPEG-dihexPLA copolymer (MW > 6000 g/mol), the diffusion of such small molecules into skin and their interaction with stratum corneum is relatively facile. As for the micelles used in the present study, it was also hypothesised that the nanoparticulate nature of the MO/oleic acid system resulted in the formation of a depot on the skin surface and in the appendages.

In conclusion, the CsA loaded micelle formulation appears to be a better delivery system than bulk MO liquid crystalline formulations [10,36]—it enables targeted delivery of CsA to skin, avoids its transdermal permeation and potential systemic exposure to the drug *in vivo*. Although cutaneous delivery of CsA from the water-rich hexagonal nano-dispersions [11] was superior this may be attributed, in part, to the effect of ethanol. It should also be noted that, in contrast to these more complex formulations, the MPEG-dihexPLA micelles have the advantage of being a "single excipient" carrier.

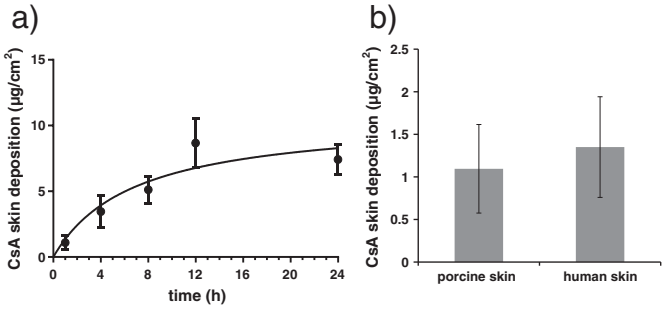

Fig. 7. a) CsA deposition as a function of application time in porcine skin (data are expressed as mean ± SD; n = 5). b) Comparison of CsA deposition in porcine and human skin after micelle application for 1 h.

3.5. Visualisation of micelle penetration pathways using Fluo-CsA loaded micelles

After the application of fluorescent micelles on porcine skin, the localisation of both Fluo-CsA and NR-MPEG-dihexPLA copolymer could be visualised using CLSM (Fig. 8).

The stability of the bond between Nile Red and the MPEG-dihexPLA copolymer was proven by mass spectroscopy and the labelled copolymer was found to be stable over the duration of the experiment, inferring that the red signal seen in the images originated specifically from the copolymer and not from the free dye. For the Fluo-CsA, some free dye was found in skin after the delivery experiment; however, this amount was considered to be negligible, as it constituted only 4% of the total fluorescein signal. It appeared that the NR-MPEG-dihexPLA copolymer remained on the skin surface (Fig. 8a), whereas Fluo-CsA penetrated into the skin (Fig. 8b and c). Given its high molecular weight (Mn of 6080 g/mol), the copolymer could not cross the stratum corneum barrier and released Fluo-CsA from the skin surface.

It has been suggested that skin structure is not entirely homogeneous and corneocytes are organised not only in parallel horizontal layers, but also in vertical columns [38–40]. A group of such columns is called a "cluster" and its boundaries form furrows that seem to match the fine wrinkles seen at the skin surface [40]. This organisation has been observed in murine [38], porcine [39] and human skins [41,42]. Confocal microscopy investigations led to the suggestion that the intercellular spaces between clusters are more permeable [38] than the traditional intercellular route between single corneocytes, especially to drugs encapsulated in colloidal systems such as vesicles and liposomes [38,39,41]. It was also recently shown that ZnO nanoparticles of a similar size to the micelles (30 nm) are preferentially deposited into inter-cluster regions (furrows) and into the orifices of the hair follicles [42].

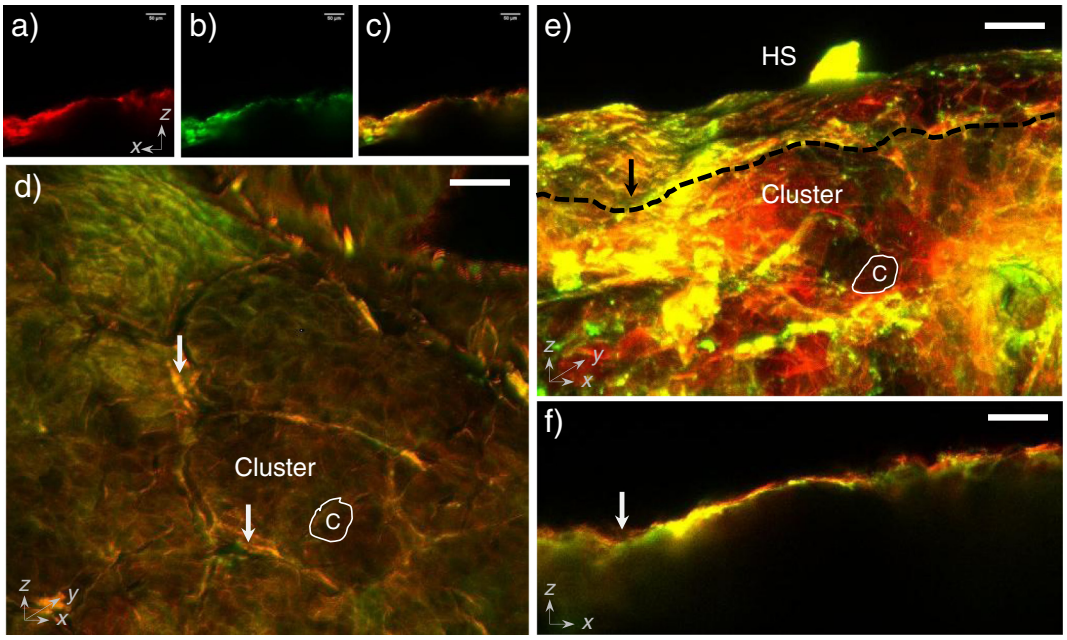

Fig. 8. Optical skin cross-sections (xz plane) with respective deposition of (a) NR-MPEG-dihexPLA copolymer, (b) Fluo-CsA and (c) superimposition of both signals. Figures (d) and (e) represent a three-dimensional reconstruction of skin surface with deposition of NR-MPEG-dihexPLA copolymer and Fluo-CsA. Corneocytes (C) can be clearly observed and appear to be organised in bigger structures denoted as "clusters". NR-MPEG-dihexPLA copolymer and Fluo-CsA seem to accumulate preferentially in regions between the clusters (inter-cluster regions) denoted by arrows. A hair shaft (HS) can be seen (e). (f) Results from an optical skin cross-section (xz plane) from (e) (denoted as dotted line): the skin penetration of Fluo-CsA seems to be deeper directly under the inter-cluster regions (arrow). Bar = 50 μm.

In the present study, CLSM three-dimensional reconstructions of the skin (Fig. 8d and e) showed several skin structures such as a hair shaft, single corneocytes and interestingly inter-cluster regions. It seems that the inter-corneocyte and inter-cluster regions are preferential micelle deposition sites, which is consistent with the observations found in the literature [38–42].

Moreover, from Fig. 8f it can be seen that Fluo-CsA penetration into skin is deeper directly under the inter-cluster regions (arrows). These findings can explain the increased CsA delivery yielded by MPEG-dihexPLA micelles in comparison to the control formulations. Like other nanoparticulate systems [40,42], micelles are probably deposited preferentially in skin wrinkles, between the corneocyte clusters, where they leverage this more permeable zone to increase drug delivery. However, as yet it is not known whether psoriatic skin possesses such histological structures and if the inter-cluster pathway is still relevant in this disease.

4. Conclusion

MPEG-dihexPLA micelles efficiently incorporated and delivered the poorly water soluble drug ciclosporin A (CsA). The nanometre-scale, spherical micelles increased the aqueous solubility of CsA by up to 518-fold. *In vitro* skin permeation experiments indicated that micelles significantly increased cutaneous bioavailability of CsA without any transdermal permeation—thus, yielding a targeted delivery to skin and minimising the risk of systemic exposure of the drug *in vivo*. Statistically equivalent supra-therapeutic amounts of CsA were delivered to porcine and human skins after application for 1 h of the formulation with the lowest CsA and copolymer content. A fluorescent analogue of CsA (Fluo-CsA) was successfully synthesised and characterised. Having a similar structure, surface lipophilicity and distribution coefficient to native CsA, Fluo-CsA was easily incorporated into fluorescent NR-MPEG-dihexPLA micelles. Fluo-CsA and the fluorescent copolymer were visualised in skin by CLSM. The images indicated that skin application of the copolymer was safe as it was unable to cross the stratum corneum. The Fluo-CsA loaded micelles appeared to be preferentially deposited in between corneocytes and in the inter-cluster regions. Fluo-CsA skin penetration was deeper under these latter structures, suggesting that this might be the preferential transport pathway responsible for the increased topical delivery of CsA yielded by micelles. This study confirms that MPEG-dihexPLA micelles are an innovative nanosized carrier able to increase topical CsA skin delivery. Although, at the outset, the aim was to develop a topical formulation that might be of interest in the treatment of psoriasis, it is clear that CsA has many other potential applications in dermatological therapy [43,44]. However, considering the histo-pathological modifications of psoriatic skin, the potential of this delivery system has to be confirmed *in vivo* with diseased skin.

Acknowledgements

We thank the University of Geneva for teaching assistantships for ML and VS. We would also like to acknowledge Dr. Christoph Bauer and Jerôme Bosset at the Bioimaging Centre of University of Geneva for their help with confocal and electron microscopy.

Appendix A. Supplementary data

Supplementary data to this article can be found online at http://dx.doi.org/10.1016/j.jconrel.2014.09.021.

References

[1] M.A. Lowes, A.M. Bowcock, J.G. Krueger, Pathogenesis and therapy of psoriasis, Nature 445 (2007) 866–873.
[2] A. Mitra, Y. Wu, Topical delivery for the treatment of psoriasis, Expert Opin. Drug Deliv. 7 (2010) 977–992.
[3] E.J. Horn, S. Domm, H.I. Katz, M. Lebwohl, U. Mrowietz, K. Kragballe, Topical corticosteroids in psoriasis: strategies for improving safety, J. Eur. Acad. Dermatol. Venereol. 24 (2010) 119–124.
[4] FDA.gov, Neoral medication guide, 2009.
[5] H. Liu, Y. Wang, Y. Lang, H. Yao, Y. Dong, S. Li, Bicontinuous cyclosporin a loaded water-AOT/Tween 85-isopropylmyristate microemulsion: structural characterization and dermal pharmacokinetics in vivo, J. Pharm. Sci. 98 (2009) 1167–1176.
[6] T. Hirano, K. Oka, Y. Umezawa, M. Hirata, T. Oh-i, M. Koga, Individual pharmacodynamics assessed by antilymphocyte action predicts clinical cyclosporine efficacy in psoriasis, Clin. Pharmacol. Ther. 63 (1998) 465–470.

[7] Y. Umezawa, T. Oh-i, M. Koga, Relationship between lymphocyte cyclosporin sensitivity and clinical progress of psoriasis, J. Dermatol. Sci. 26 (2001) 94–99.
[8] H. Liu, S. Li, Y. Wang, F. Han, Y. Dong, Bicontinuous water-AOT/Tween85-isopropyl myristate microemulsion: a new vehicle for transdermal delivery of cyclosporin A, Drug. Dev. Ind. Pharm. 32 (2006) 549–557.
[9] H. Liu, Y. Wang, F. Han, H. Yao, S. Li, Gelatin-stabilised microemulsion-based organogels facilitates percutaneous penetration of Cyclosporin A in vitro and dermal pharmacokinetics in vivo, J. Pharm. Sci. 96 (2007) 3000–3009.
[10] L.B. Lopes, J.L. Lopes, D.C. Oliveira, J.A. Thomazini, M.T. Garcia, M.C. Fantini, J.H. Collett, M.V. Bentley, Liquid crystalline phases of monoolein and water for topical delivery of cyclosporin A: characterization and study of in vitro and in vivo delivery, Eur. J. Pharm. Biopharm. 63 (2006) 146–155.
[11] L.B. Lopes, D.A. Ferreira, D. de Paula, M.T. Garcia, J.A. Thomazini, M.C. Fantini, M.V. Bentley, Reverse hexagonal phase nanodispersion of monoolein and oleic acid for topical delivery of peptides: in vitro and in vivo skin penetration of cyclosporin A, Pharm. Res. 23 (2006) 1332–1342.
[12] V. Prasad, N. Kumar, P.R. Mishra, Amphiphilic gels as a potential carrier for topical drug delivery, Drug Deliv. 14 (2007) 75–85.
[13] S.T. Kim, D.J. Jang, J.H. Kim, J.Y. Park, J.S. Lim, S.Y. Lee, K.M. Lee, S.J. Lim, C.K. Kim, Topical administration of cyclosporin A in a solid lipid nanoparticle formulation, Pharmazie 64 (2009) 510–514.
[14] T. Trimaille, K. Mondon, R. Gurny, M. Moller, Novel polymeric micelles for hydrophobic drug delivery based on biodegradable poly(hexyl-substituted lactides), Int. J. Pharm. 319 (2006) 147–154.
[15] K. Mondon, M. Zeisser-Labouebe, R. Gurny, M. Moller, Novel cyclosporin A formulations using MPEG-hexyl-substituted polylactide micelles: a suitability study, Eur. J. Pharm. Biopharm. 77 (2011) 56–65.
[16] T. Trimaille, R. Gurny, M. Moller, Poly(hexyl-substituted lactides): novel injectable hydrophobic drug delivery systems, J. Biomed. Mater. Res. A 80A (2007) 55–65.
[17] C. Di Tommaso, F. Behar-Cohen, R. Gurny, M. Moller, Colloidal systems for the delivery of cyclosporin A to the anterior segment of the eye, Ann. Pharm. Fr. 69 (2011) 116–123.
[18] C. Di Tommaso, C. Como, R. Gurny, M. Moller, Investigations on the lyophilisation of MPEG-hexPLA micelle based pharmaceutical formulations, Eur. J. Pharm. Sci. 40 (2010) 38–47.
[19] C.D.T.G. Trubitsyn, R. Gurny, M. Möller, Novel PEG-hexPLA micellar drug carriers with a covalently labeled Nile Red fluorescence marker, PolyColl, 2011, (Geneva).
[20] S. Gaali, C. Kozany, B. Hoogeland, M. Klein, F. Hausch, Facile synthesis of a fluorescent cyclosporin a analogue to study cyclophilin 40 and cyclophilin 18 ligands, ACS Med. Chem. Lett. 1 (2010) 536–539.
[21] W. Humphrey, A. Dalke, K. Schulten, VMD: visual molecular dynamics, J. Mol. Graph. 14 (1996) 33–38 (27–38).
[22] OECD Guidelines for the Testing of Chemicals, Test No. 107: Partition Coefficient (n-octanol/water): Shake Flask Method, OECD, 1995.
[23] Validation of Analytical Procedures: Text and Methodology Topic Q 2 (R1), International Conference on Harmonisation of Technical Requirments for registration of Pharmaceuticals for Human Use, 2005.
[24] Guidance for Industry, Bioanalytical Method Validation, in: U.S. Department of Health and Human Services (Ed.), Food and Drug Adminstration, 2001.
[25] K. Mondon, M. Zeisser-Labouebe, R. Gurny, M. Möller, MPEG-hexPLA micelles as novel carriers for hypericin, a fluorescent marker for use in cancer diagnostics, Photochem. Photobiol. 87 (2011) 399–407.
[26] Y.G. Bachhav, K. Mondon, Y.N. Kalia, R. Gurny, M. Moller, Novel micelle formulations to increase cutaneous bioavailability of azole antifungals, J. Control. Release 153 (2011) 126–132.
[27] I.P. Dick, R.C. Scott, Pig ear skin as an in-vitro model for human skin permeability, J. Pharm. Pharmacol. 44 (1992) 640–645.
[28] U. Jacobi, M. Kaiser, R. Toll, S. Mangelsdorf, H. Audring, N. Otberg, W. Sterry, J. Lademann, Porcine ear skin: an in vitro model for human skin, Skin Res. Technol. 13 (2007) 19–24.
[29] F.P. Schmook, J.G. Meingassner, A. Billich, Comparison of human skin or epidermis models with human and animal skin in in-vitro percutaneous absorption, Int. J. Pharm. 215 (2001) 51–56.
[30] Scifinder, Calculated using Advanced Chemistry Development, (ACD/Labs) Software V11.02, (© 1994-2013 ACD/Labs) 4 (2014).
[31] D. Margulies, G. Melman, A. Shanzer, Fluorescein as a model molecular calculator with reset capability, Nat. Mater. 4 (2005) 768–771.
[32] H. Lambers, S. Piessens, A. Bloem, H. Pronk, P. Finkel, Natural skin surface pH is on average below 5, which is beneficial for its resident flora, Int. J. Cosmet. Sci. 28 (2006) 359–370.
[33] J. Liaw, Y. Lin, Evaluation of poly(ethylene oxide)-poly(propylene oxide)-poly(ethylene oxide) (PEO-PPO-PEO) gels as a release vehicle for percutaneous fentanyl, J. Control. Release 68 (2000) 273–282.
[34] P.L. Honeywell-Nguyen, A.M. de Graaff, H.W. Groenink, J.A. Bouwstra, The in vivo and in vitro interactions of elastic and rigid vesicles with human skin, Biochim. Biophys. Acta 1573 (2002) 130–140.
[35] H. Wagner, K.H. Kostka, C.M. Lehr, U.F. Schaefer, Drug distribution in human skin using two different in vitro test systems: comparison with in vivo data, Pharm. Res. 17 (2000) 1475–1481.
[36] L.B. Lopes, J.H. Collett, M.V. Bentley, Topical delivery of cyclosporin A: an in vitro study using monoolein as a penetration enhancer, Eur. J. Pharm. Biopharm. 60 (2005) 25–30.
[37] A. Ganem-Quintanar, D. Quintanar-Guerrero, P. Buri, Monoolein: a review of the pharmaceutical applications, Drug Dev. Ind. Pharm. 26 (2000) 809–820.
[38] A. Schatzlein, G. Cevc, Non-uniform cellular packing of the stratum corneum and permeability barrier function of intact skin: a high-resolution confocal laser scanning microscopy study using highly deformable vesicles (Transfersomes), Br. J. Dermatol. 138 (1998) 583–592.
[39] D.C. Carrer, C. Vermehren, L.A. Bagatolli, Pig skin structure and transdermal delivery of liposomes: a two photon microscopy study, J. Control. Release 132 (2008) 12–20.
[40] G. Cevc, U. Vierl, Nanotechnology and the transdermal route: a state of the art review and critical appraisal, J. Control. Release 141 (2010) 277–299.
[41] M.E. van Kuijk-Meuwissen, H.E. Junginger, J.A. Bouwstra, Interactions between liposomes and human skin in vitro, a confocal laser scanning microscopy study, Biochim. Biophys. Acta 1371 (1998) 31–39.
[42] M.E. Darvin, K. Konig, M. Kellner-Hoefer, H.G. Breunig, W. Werncke, M.C. Meinke, A. Patzelt, W. Sterry, J. Lademann, Safety assessment by multiphoton fluorescence/second harmonic generation/hyper-Rayleigh scattering tomography of ZnO nanoparticles used in cosmetic products, Skin Pharmacol. Physiol. 25 (2012) 219–226.
[43] K.T. Amor, C. Ryan, A. Menter, The use of cyclosporine in dermatology: part I, J. Am. Acad. Dermatol. 63 (2010) 925–946 (quiz 947-928).
[44] C. Ryan, K.T. Amor, A. Menter, The use of cyclosporine in dermatology: part II, J. Am. Acad. Dermatol. 63 (2010) 949–972 (quiz 973-944).